



Dolosigranulum pigrum Cooperation and Competition in Human Nasal Microbiota

Silvio D. Brugger,^{a,b,c} Sara M. Eslami,^b Melinda M. Pettigrew,^d Isabel F. Escapa,^{b,c,e} Matthew T. Henke,^f Yong Kong,^g
 Katherine P. Lemon^{b,e,h,i}

^aDepartment of Infectious Diseases and Hospital Epidemiology, University Hospital Zurich, University of Zurich, Zurich, Switzerland

^bThe Forsyth Institute (Microbiology), Cambridge, Massachusetts, USA

^cDepartment of Oral Medicine, Infection and Immunity, Harvard School of Dental Medicine, Boston, Massachusetts, USA

^dDepartment of Epidemiology of Microbial Diseases, Yale School of Public Health, New Haven, Connecticut, USA

^eAlkek Center for Metagenomics & Microbiome Research, Department of Molecular Virology & Microbiology, Baylor College of Medicine, Houston, Texas, USA

^fDepartment of Biological Chemistry and Molecular Pharmacology, Harvard Medical School, Boston, Massachusetts, USA

^gDepartment of Molecular Biophysics and Biochemistry and W.M. Keck Foundation Biotechnology Resource Laboratory, Yale University, New Haven, Connecticut, USA

^hDivision of Infectious Diseases, Boston Children's Hospital, Harvard Medical School, Boston, Massachusetts, USA

ⁱSection of Infectious Diseases, Department of Pediatrics, Texas Children's Hospital and Baylor College of Medicine, Houston, Texas, USA

Silvio D. Brugger, Sara M. Eslami, and Melinda M. Pettigrew contributed equally to this article, and authorship order was decided based on a combination of the specific type of contribution and seniority within the collaborating research groups.

ABSTRACT Multiple epidemiological studies identify *Dolosigranulum pigrum* as a candidate beneficial bacterium based on its positive association with health, including negative associations with nasal/nasopharyngeal colonization by the pathogenic species *Staphylococcus aureus* and *Streptococcus pneumoniae*. Using a multipronged approach to gain new insights into *D. pigrum* function, we observed phenotypic interactions and predictions of genomic capacity that support the idea of a role for microbe-microbe interactions involving *D. pigrum* in shaping the composition of human nasal microbiota. We identified *in vivo* community-level and *in vitro* phenotypic cooperation by specific nasal *Corynebacterium* species. Also, *D. pigrum* inhibited *S. aureus* growth *in vitro*, whereas robust inhibition of *S. pneumoniae* required both *D. pigrum* and a nasal *Corynebacterium* together. *D. pigrum* L-lactic acid production was insufficient to account for these inhibitions. Genomic analysis of 11 strains revealed that *D. pigrum* has a small genome (average 1.86 Mb) and multiple predicted auxotrophies consistent with *D. pigrum* relying on its human host and on cocolonizing bacteria for key nutrients. Further, the accessory genome of *D. pigrum* harbored a diverse repertoire of biosynthetic gene clusters, some of which may have a role in microbe-microbe interactions. These new insights into *D. pigrum*'s functions advance the field from compositional analysis to genomic and phenotypic experimentation on a potentially beneficial bacterial resident of the human upper respiratory tract and lay the foundation for future animal and clinical experiments.


IMPORTANCE *Staphylococcus aureus* and *Streptococcus pneumoniae* infections cause significant morbidity and mortality in humans. For both, nasal colonization is a risk factor for infection. Studies of nasal microbiota identify *Dolosigranulum pigrum* as a benign bacterium present when adults are free of *S. aureus* or when children are free of *S. pneumoniae*. Here, we validated these *in vivo* associations with functional assays. We found that *D. pigrum* inhibited *S. aureus* *in vitro* and, together with a specific nasal *Corynebacterium* species, also inhibited *S. pneumoniae*. Furthermore, genomic analysis of *D. pigrum* indicated that it must obtain key nutrients from other nasal bacteria or from humans. These phenotypic interactions support the idea of a role for microbe-microbe interactions in shaping the composition of

Citation Brugger SD, Eslami SM, Pettigrew MM, Escapa IF, Henke MT, Kong Y, Lemon KP. 2020. *Dolosigranulum pigrum* cooperation and competition in human nasal microbiota. mSphere 5:e00852-20. <https://doi.org/10.1128/mSphere.00852-20>.

Editor Sarah E. F. D'Orazio, University of Kentucky

Copyright © 2020 Brugger et al. This is an open-access article distributed under the terms of the [Creative Commons Attribution 4.0 International license](https://creativecommons.org/licenses/by/4.0/).

Address correspondence to Silvio D. Brugger, silvio.brugger@usz.ch, or Katherine P. Lemon, katherine.lemon@bcm.edu.

 *Dolosigranulum pigrum* Cooperation and Competition in Human Nasal Microbiota @KLemonLab

Received 21 August 2020

Accepted 24 August 2020

Published 9 September 2020

human nasal microbiota and implicate *D. pigrum* as a mutualist of humans. These findings support the feasibility of future development of microbe-targeted interventions to reshape nasal microbiota composition to exclude *S. aureus* and/or *S. pneumoniae*.

KEYWORDS *Dolosigranulum pigrum*, *Corynebacterium*, *Staphylococcus aureus*, *Streptococcus pneumoniae*, microbe-microbe interactions, interspecies interactions, upper respiratory tract, nasal, microbiota, comparative genomics

Colonization of the human nasal passages by *Staphylococcus aureus* or *Streptococcus pneumoniae* is a major risk factor for infection by the colonizing bacterium at a distant body site (1–5). Interventions that reduce the prevalence of colonization also reduce the risk of infection and transmission (6, 7). *S. aureus* and *S. pneumoniae* are major human pathogens that cause significant morbidity and mortality worldwide (8–11). There are also concerns regarding rising rates of antimicrobial resistance (12) and the potential for long-term effects of antibiotics early in life (13). Thus, efforts have recently focused on the identification of candidate bacteria that confer colonization resistance against *S. aureus* (14–21) and *S. pneumoniae* (22–25), with particular urgency for *S. aureus* in the absence of an effective vaccine.

Dolosigranulum pigrum has emerged in multiple studies of the human upper respiratory tract (URT) microbiota, colonizing with or without *Corynebacterium* species, as potentially beneficial and/or protective against colonization by *S. aureus* and *S. pneumoniae* (26–53) (reviewed in references 14, 54, 55, 56, and 57). However, little is known about this Gram-positive, catalase-negative, *Firmicute* bacterium, first described in 1993 (58). Microbiota studies sampling either nostrils or nasopharynx have shown very similar results; therefore, for simplicity, we use “nasal” or “nasal passages” to denote the area inclusive of the nostrils through the nasopharynx. *D. pigrum* and *S. aureus* are inversely correlated in adult nasal microbiota (30, 41, 59), whereas, in pediatric nasal microbiota, *D. pigrum* and members of the genus *Corynebacterium* are overrepresented when *S. pneumoniae* is absent (26, 33). Moreover, children with *D. pigrum* colonization of the nasal passages are less likely to have acute otitis media (27, 40) and it has been speculated that *D. pigrum*-dominated microbiota profiles might be more resistant to invasive pneumococcal disease (46). Furthermore, *D. pigrum* abundance in the nasal passages is inversely associated with wheezing and respiratory tract infections in infants (28) and an abundance of *D. pigrum* with *Corynebacterium* in adults provides greater community stability in the face of pneumococcal exposure (51). The intriguing inference from these studies that *D. pigrum* plays a beneficial role in human nasal microbiota deserves further investigation.

In contrast to the data mentioned above, there are very few reports of *D. pigrum* in association with human disease (60–68). Its frequent identification in human nasal microbiota (26–53, 69–81) and its rare association with infection are consistent with *D. pigrum* functioning as a commensal and, possibly, as a mutualist of humans—characteristics that support the idea of its potential for future use as a therapeutic. However, its metabolism and its interplay with other nasal bacteria remain uncharted territory. Using a multipronged approach, we have made significant advances in these areas. First, we identified specific species of candidate bacterial interactors with *D. pigrum* by analyzing nasal microbiota data sets from adults and children. Second, we used *in vitro* phenotypic assays to show that *D. pigrum* exhibits distinct interaction phenotypes with nasal *Corynebacterium* species, *S. aureus*, and *S. pneumoniae*. Third, on the basis of the genomes of 11 distinct *D. pigrum* strains, we identify key predicted functions and auxotrophies in its core genome plus a diversity of predicted biosynthetic gene clusters (BCGs) in its accessory genome. This critical shift to phenotypic and genomic experimentation marks a significant advance in understanding *D. pigrum*, a potentially beneficial member of human nasal microbiota.

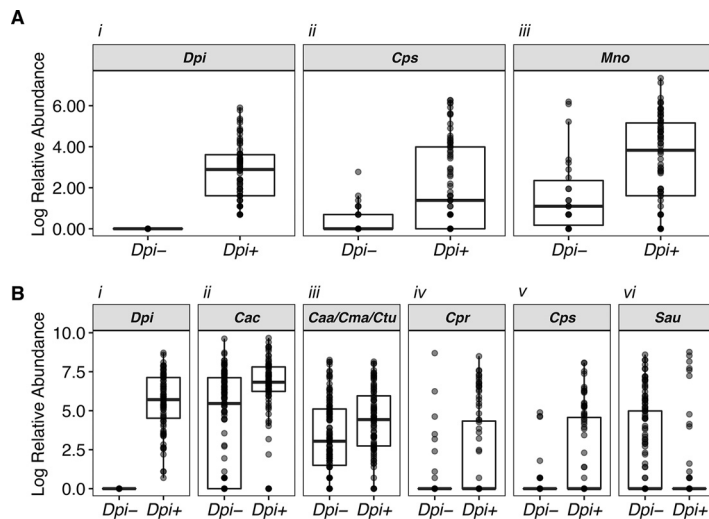


FIG 1 Individual nasal *Corynebacterium* species exhibit increased differential relative abundances in the presence of *D. pigrum* in human nostril microbiota. We used ANCOM to compare the species/supraspecies-level compositions of 16S rRNA gene nostril data sets from (A) 99 children ages 6 to 78 months and (B) 210 adults where *D. pigrum* was either absent (*Dpi*⁻) or present (*Dpi*⁺) on the basis of 16S rRNA gene sequencing data. Plots show only the taxa identified as statistically significant ($\text{sig} = 0.05$) after correction for multiple testing within ANCOM. The dark bar represents the median; lower and upper hinges correspond to the first and third quartiles. Each gray dot represents the value for a sample, and multiple overlapping dots appear black. *Dpi* = *Dolosigranulum pigrum*, *Cac* = *Corynebacterium accolens*, *Caa/Cma/Ctu* = supraspecies *Corynebacterium accolens_macginleyi_tuberculostearicum*, *Cpr* = *Corynebacterium propinquum*, *Cps* = *Corynebacterium pseudodiphtheriticum*, *Mno* = *Moraxella nonliquefaciens*. Only three species and one supraspecies of *Corynebacterium* from among the larger number of *Corynebacterium* supraspecies/species present in each data set met the significance threshold. Specifically, in the adult nostril data set, there were 21 species and 5 supraspecies groupings of *Corynebacterium* in addition to the reads of *Corynebacterium* that were nonassigned (NA) at the species level. These data were previously published (see Table S7 in reference 41). In the pediatric data set, there were 16 species of *Corynebacterium* in addition to those that were nonassigned among the species-level *Corynebacterium* reads (see Table S2). The Log relative abundance numerical data represented in this figure are available in Table S1.

RESULTS

Individual bacterial species are associated with *D. pigrum* in the nasal microbiota of both adults and children. *D. pigrum* is the only member of its genus, and multiple 16S rRNA gene-based nasal microbiota studies have identified associations between *Dolosigranulum* and other genera, such as *Corynebacterium* (see, e.g., references 28, 29, 31, 36, 38, 40, 41, 43, and 82). In most cases, the taxonomic resolution in the aforementioned studies was limited to the genus or higher taxonomic levels. Thus, we sought to achieve finer taxonomic resolution and to determine which species are associated with *D. pigrum*. We identified two nostril data sets with V1-V2/V1-V3 16S rRNA gene sequences, regions that contain sufficient information for species-level taxonomic assignment of most nose-associated bacteria (26, 41). After parsing sequences into species-level phylotypes, we interrogated each data set using analysis of composition of microbiomes (ANCOM) (83) to identify bacterial species that display differential relative abundances in the absence or presence of *D. pigrum* sequences (Fig. 1; see also Table S1 in the supplemental material). In the nostrils of 99 children ages 6 to 78 months (26), *Corynebacterium pseudodiphtheriticum* exhibited increased differential relative abundance in the presence of *D. pigrum*, i.e., was positively associated with *D. pigrum*, as was *Moraxella nonliquefaciens* (Fig. 1A). In the nostrils of 210 adults from the Human Microbiome Project (HMP), three *Corynebacterium* species—*Corynebacterium accolens*, *C. propinquum*, and *C. pseudodiphtheriticum*—and an unresolved supraspecies of *C. accolens_macginleyi_tuberculostearicum* were positively associated with *D. pigrum* (Fig. 1B, panels ii to v), whereas *S. aureus* was negatively associated with *D. pigrum* (Fig. 1B, panel vi). The associations identified in compositional microbiota data observed here and in prior studies (28, 29, 31, 36, 38, 40, 41, 43,

82) led to testable hypotheses about possible direct microbe-microbe interactions between *D. pigrum* and the specific nasal *Corynebacterium* species, as well as between *D. pigrum* and *S. aureus*. Therefore, we used *in vitro* phenotypic assays to test our hypotheses about direct microbe-microbe interactions.

Nasal *Corynebacterium* species can enhance the growth of *D. pigrum* *in vitro*.

We hypothesized that the strong positive association between *D. pigrum* and the nasal passage-associated *Corynebacterium* species might be due to these *Corynebacterium* species releasing metabolites that enhance the growth of *D. pigrum*. To test this, we quantified *D. pigrum* growth yields on unconditioned agar medium compared to the yields seen on cell-free agar medium conditioned by growth of *C. pseudodiphtheriticum*, *C. propinquum*, or *C. accolens* (Fig. 2). Conditioning agar medium by prior growth of any of these three nasal *Corynebacterium* species increased the yield (measured as CFU) of two *D. pigrum* strains (CDC4709-98 and KPL1914) by 1 to 2 orders of magnitude compared to growth on unconditioned agar medium (Fig. 2A and B). Additionally, one strain of *C. pseudodiphtheriticum* (Fig. 2A) and the *C. accolens* strain (Fig. 2B) increased the growth yield of *D. pigrum* CDC2949-98, a strain with a higher baseline growth yield. The increases in *D. pigrum* growth yield on *Corynebacterium* cell-free conditioned agar medium (CFCAM) might have resulted from increased growth rate or increased viability or both and might be consistent with the nasal *Corynebacterium* species either removing a toxin from the medium or releasing a metabolite that enhances growth and/or survival of *D. pigrum*.

In contrast to the increase in *D. pigrum* growth yield on *C. pseudodiphtheriticum* CFCAM (Fig. 2A), there was no increase in *C. pseudodiphtheriticum* strain KPL1989 growth yield on *D. pigrum* CFCAM (Fig. 2C). Thus, this growth enhancement goes in one direction from nasal *Corynebacterium* species to *D. pigrum*. This is consistent with unilateral cooperation of nasal *Corynebacterium* species—*C. pseudodiphtheriticum*, *C. propinquum* or *C. accolens*—with *D. pigrum* in the nostril microbiota and supports the observed positive *in vivo* community-level relationships (Fig. 1).

The positive association between *C. accolens* and *D. pigrum* in adult nostril microbiota data sets indicates that *in vivo* positive interactions between *C. accolens* and *D. pigrum* prevail (Fig. 1B, panel ii). However, *in vitro*, we observed either a positive or a negative interaction between *C. accolens* and *D. pigrum* depending on the assay conditions. *C. accolens*, unlike *C. propinquum* and *C. pseudodiphtheriticum*, is a fatty acid auxotroph, and triolein, a model host epithelial-surface triacylglycerol, served as a source of needed oleic acid in our assays. We observed increased *D. pigrum* growth yield on a semipermeable membrane atop *C. accolens* CFCAM consisting of brain heart infusion (BHI) agar supplemented with triolein (BHIT) (Fig. 2B). In contrast, *D. pigrum* was inhibited when placed directly onto this same *C. accolens* CFCAM (Table 1). This inhibition is reminiscent of our previous finding that the *C. accolens* triacylglycerol lipase LipS1 hydrolyzes triacylglycerols, releasing free fatty acids that inhibit *S. pneumoniae* (33), and *S. pneumoniae* served as a positive control for the effect of *C. accolens* in this assay (Table 1). Both *D. pigrum* and *S. pneumoniae* belong to the order *Lactobacillales*, and we hypothesized that *D. pigrum* might be similarly susceptible to free fatty acids such as the oleic acid that *C. accolens* releases from triolein. Indeed, we observed that oleic acid inhibited *D. pigrum* when we challenged *D. pigrum* with oleic acid using a disk diffusion assay with *S. pneumoniae* as a positive control (Table 2). We also challenged *D. pigrum* with various concentrations of oleic acid spread onto plates of BHI agar medium. Similarly to the membrane-mediated effect seen in the *C. accolens* CFCAM experiment described above, we observed *D. pigrum* growth at higher concentrations of oleic acid when it was placed on a semipermeable membrane atop the oleic acid-coated medium than when it was placed directly on the oleic acid-coated medium (Table 3). This indicates that the membrane provided some protection from inhibition by oleic acid. Overall, these *in vitro* data indicate that *C. accolens* can both inhibit the growth of *D. pigrum* by releasing antibacterial-free fatty acids from host triacylglycerols, such as oleic acid from triolein (Tables 1 and 2), and enhance the growth of *D. pigrum* by releasing an as-yet-unidentified factor(s) (Fig. 2B). Collectively,

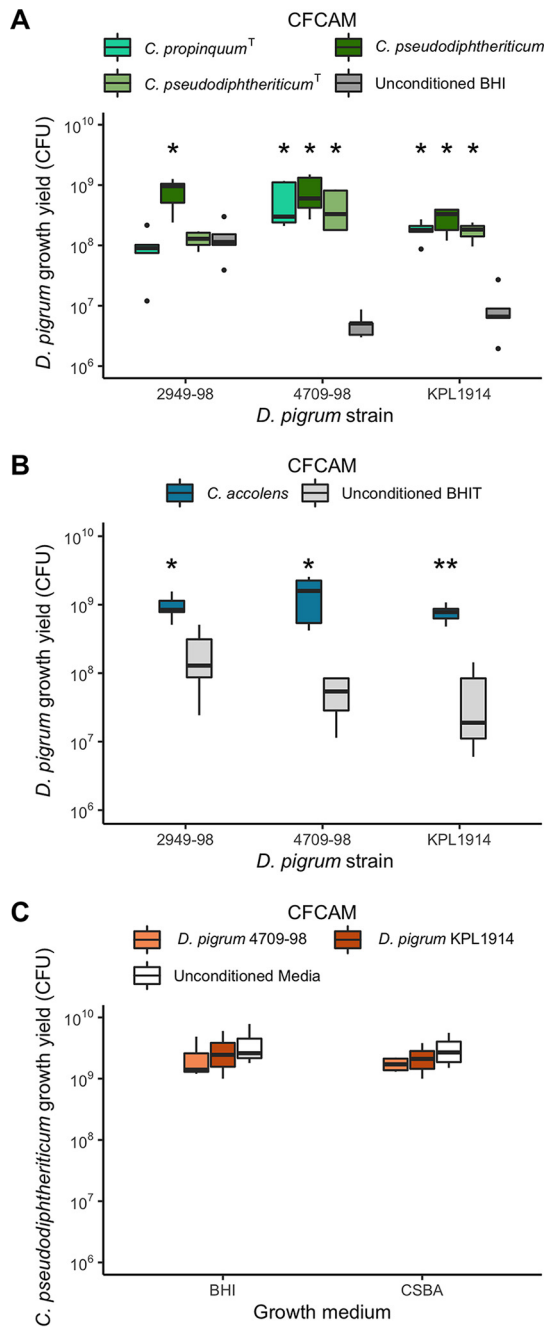


FIG 2 *D. pigrum* growth yields increase on cell-free conditioned agar medium (CFCAM) from nasal *Corynebacterium* species but not in reverse. (A and B) Growth yield of *D. pigrum* strains CDC2949-98, CDC4709-98, and KPL1914 was quantified as the number of CFU grown on a polycarbonate membrane placed on (A) cell-free conditioned BHI agar from *C. propinquum* (aqua green) or *C. pseudodiphtheriticum* (dark and light green) or (B) cell-free conditioned BHI-triolein (BHIT) agar from *C. accolens* (blue) and compared to growth on unconditioned BHI agar (dark gray) or unconditioned BHIT agar (light gray), respectively. (C) Growth yield of *C. pseudodiphtheriticum* KPL1989 on CFCAM from *D. pigrum* strains (orange) compared to unconditioned medium (white) was assessed similarly. BHIT was used for growth of *C. accolens* since it is a fatty acid auxotroph and releases needed oleic acid from triolein. Preconditioning strains were grown on a 0.2- μ m-pore-size, 47-mm-diameter polycarbonate membrane for 2 days to generate CFCAM. After removal, we then placed a new membrane on the CFCAM onto which we spread 100 μ l of target bacterial cells that had been resuspended to an OD₆₀₀ of 0.50 in 1 \times PBS. After 2 days of growth, CFU were enumerated as described in Materials and Methods. CFU counts were compared independently for each individual strain (A and B, $n = 5$) or medium (C, $n = 4$) using a Wilcoxon rank sum test with Bonferroni correction for multiple comparisons to the unconditioned medium. Dark bars represent medians, lower and upper hinges correspond to the first and third quartiles, and outlier points are displayed individually. *, $P \leq 0.05$; **, $P \leq 0.001$. CSBA, citrated sheep blood agar.

TABLE 1 In contrast to growth on a semipermeable membrane, *D. pigrum* is inhibited when grown directly on cell-free *C. accolens*-conditioned BHI agar supplemented with triolein as a source of oleic acid

Conditioning strain	Growth of target strain ^a		
	<i>S. pneumoniae</i> 603 (6B)	<i>D. pigrum</i> CDC4709-98	<i>D. pigrum</i> KPL1914
<i>C. accolens</i> KPL1818	0	0	0
<i>C. propinquum</i> ^T DSM44285	0	+	+
<i>C. pseudodiphtheriticum</i> KPL1989	+	+	+

^a0, no growth; +, growth detected, $n \geq 3$.

these results point to a complex set of molecular interactions between these two species.

***D. pigrum* inhibits *S. aureus* growth.** The ANCOM of the adult nostril microbiota data set revealed a negative association between *S. aureus* and *D. pigrum* (Fig. 1B, panel vi). Direct antagonism would be the simplest mechanism underpinning this observation. Therefore, we assayed for the effect of 10 different strains of *D. pigrum* on *S. aureus*. We gave *D. pigrum* a head start to compensate for its lower growth rate *in vitro*. *S. aureus* growth was inhibited when it was inoculated adjacent to a pregrown inoculum of each of these 10 *D. pigrum* strains on agar medium (Fig. 3A). In contrast, a pregrown inoculum of *S. aureus* did not inhibit *D. pigrum* (Fig. 3B). Furthermore, comparing three representative *D. pigrum* strains, none of the *D. pigrum* strains, when pregrown, inhibited the other *D. pigrum* strains (Fig. 3C).

***D. pigrum* production of lactic acid is unlikely to be the primary mechanism for negative associations with *S. pneumoniae* or *S. aureus*.** *D. pigrum* lactic acid production has been proposed as a mechanism to explain epidemiologic observations of negative associations between *D. pigrum* and *S. pneumoniae* (82). Under nutrient-rich conditions *in vitro*, three tested strains of *D. pigrum* produced from 5.7 to 8.2 mM L-lactic acid, with strain KPL1914 producing the highest concentration (Fig. 4A). Therefore, we assayed for growth of *S. pneumoniae* in *D. pigrum* KPL1914 cell-free conditioned medium (CFCM) and in BHI broth supplemented with various concentrations of L-lactic acid. Three of the four *S. pneumoniae* strains tested showed some growth in 22 mM lactic acid (Fig. 4B), and all strains displayed more growth in BHI medium supplemented with 11 mM L-lactic acid than in the *D. pigrum* KPL1914 CFCM, which had 7.5 mM *D. pigrum*-produced L-lactic acid (Fig. 4B). Furthermore, growth of *S. pneumoniae* alone under these conditions resulted in a higher concentration of L-lactic acid than did *D. pigrum* growth (see Fig. S1 in the supplemental material). Thus, the restriction of *S. pneumoniae* growth in *D. pigrum* CFCM is unlikely to have been due to production of lactic acid by *D. pigrum*. More likely, it reflected competition for nutrients since fresh medium was not added to the CFCM, which, therefore, would have a lower concentration of sugars than BHI broth. However, the possibility of *D. pigrum* production of a toxin and/or an antipneumococcal compound in BHI broth cannot be excluded. We also tested the *in vitro* effect of L-lactic acid on two strains of *S. aureus*. Both showed some growth in 33 mM lactic acid (Fig. 4C). Thus, *D. pigrum* did not produce enough L-lactic acid to restrict *S. aureus* growth under the tested conditions.

TABLE 2 Oleic acid inhibits *D. pigrum* growth

Oleic acid concn ($\mu\text{g}/\text{disc}$)	ZOI (mm) ^a		
	<i>S. pneumoniae</i> 603 (6B)	<i>D. pigrum</i> CDC4709-98	<i>D. pigrum</i> KPL1914
20	10.3 \pm 4.7	12.0 \pm 2.9	17.0 \pm 2.1
50	22.0 \pm 5.4	26.8 \pm 4.4	28.4 \pm 7.0
100	26.3 \pm 6.7	35.8 \pm 4.5	39.4 \pm 5.0

^aMean zone of inhibition (ZOI) \pm standard deviation (SD) produced in a disc diffusion assay. ZOIs were measured as the smallest diameter of inhibited growth, and measurements included disc diameter (6 mm). Results from biological replicates ($n = 4$ for *S. pneumoniae*, $n = 5$ for *D. pigrum*) were averaged.

TABLE 3 A 0.2- μ m-pore-size, 47-mm-diameter polycarbonate membrane provides *D. pigrum* with some protection against inhibition by oleic acid *in vitro*^a

Plated vol of oleic acid (μ g)	Result for indicated <i>D. pigrum</i> strain			
	Growth directly on agar		Growth on membrane	
	KPL1914	CDC4709-98	KPL1914	CDC4709-98
500	0	0	0	+
50	0	0	+	+
5	+	+	+	+
0.5	+	+	+	+
0.05	+	+	+	+
0 (BHI agar)	+	+	+	+
0 (CSBA)	+	+	+	+

^a0, no growth; +, growth detected; *n* = 3. CSBA, citrated sheep blood agar.

Furthermore, growth of *S. aureus* alone resulted in a concentration of L-lactic acid similar to that seen with *D. pigrum* growth (Fig. S1). In contrast to the *S. pneumoniae* results, we would not expect depletion of sugars to have a large effect on *S. aureus* growth in *D. pigrum* CFM given its ability to utilize a broader repertoire of energy sources, e.g., amino acids. Indeed, both *S. aureus* strains showed only a minimal decrease in growth in *D. pigrum* CFM. This also revealed differences in *D. pigrum* production of the anti-*S. aureus* activity during growth on BHI agar medium (Fig. 3) versus growth in BHI broth (Fig. 4C). Levels of excretion of metabolites may differ during growth in liquid versus on agar medium, and the mechanism of the *D. pigrum* anti-*S. aureus* activity is yet to be identified.

***D. pigrum* and *C. pseudodiphtheriticum* inhibit *S. pneumoniae* growth together but not alone.** Since the effects seen with *C. pseudodiphtheriticum* were positively associated with the presence of *D. pigrum* (Fig. 1), we investigated their combined effects on *S. pneumoniae* growth. Agar medium conditioned with a coculture of *C. pseudodiphtheriticum* strain KPL1989 and *D. pigrum* strain CDC4709-98 inhibited *S. pneumoniae* growth, whereas agar medium conditioned with a monoculture of either *C. pseudodiphtheriticum* or *D. pigrum* alone did not (Fig. 5; see also Fig. S2). This might have been due to cocultivation resulting either in a greater level of nutrient competition than monoculture of either commensal alone or in the production of a diffusible

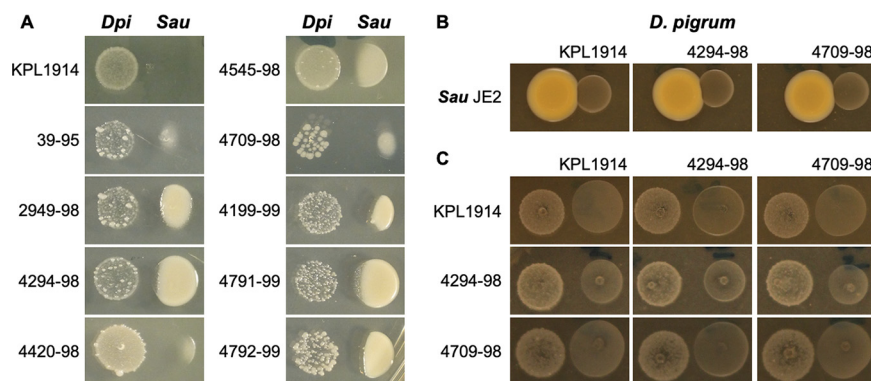


FIG 3 Ten different strains of *D. pigrum* inhibit methicillin-resistant *S. aureus* USA300 strain JE2 whereas *S. aureus* does not inhibit *D. pigrum*. (A) Ten pregrown *D. pigrum* isolates produced a diffusible activity that inhibited the growth of *S. aureus* strain JE2. (B) When *S. aureus* was pregrown in this assay, there was no visible inhibition of subsequently inoculated *D. pigrum*. (C) Similarly, we did not observe any inhibition in a pairwise comparison of three representative strains of *D. pigrum* in this assay. All growth was on BHI agar in the independent experiments (*n* \geq 3) represented in panels A, B, and C. Representative images are shown for each strain. The respective pregrown strain (*D. pigrum* or *S. aureus*) was resuspended in PBS, and then a 5- μ l drop was placed on BHI agar and pregrown for 48 h (*D. pigrum*) or 24 h (*S. aureus*). After that, the indicator strain was inoculated at a location adjacent to the pregrown strain. Inhibition was assessed after 24 and 48 h (48-h results are shown here). For panels A and B, similar results were observed using *S. aureus* Newman.

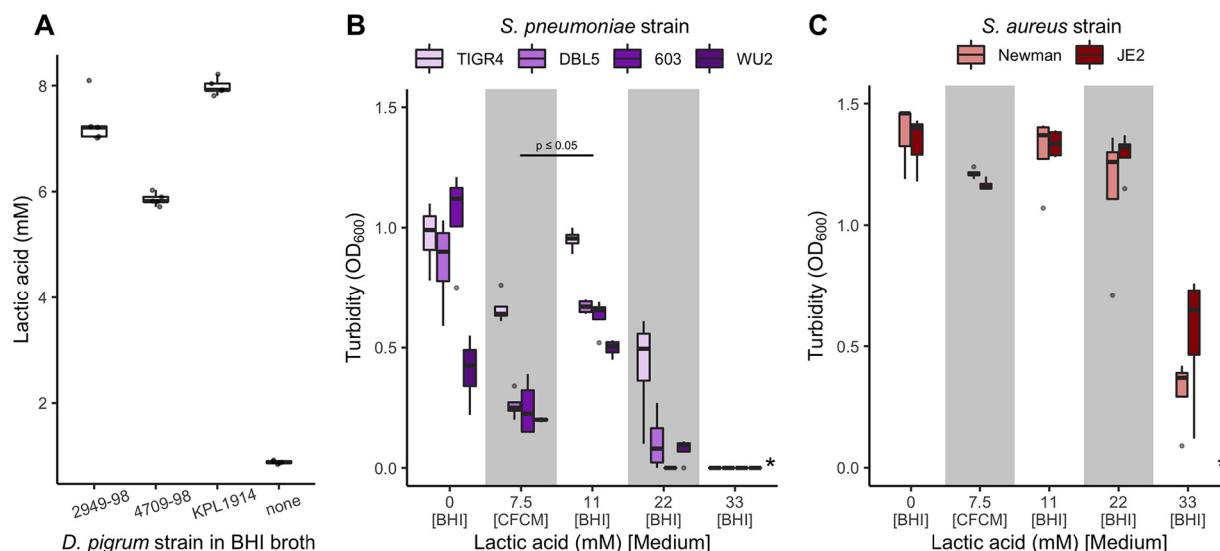


FIG 4 Lactate production by *D. pigrum* is insufficient to inhibit pathobiont growth. Strains of *S. pneumoniae* and *S. aureus* grew in the presence of higher levels of L-lactic acid than those produced by *D. pigrum* *in vitro*. (A) The concentration of L-lactic acid (mM) produced by three *D. pigrum* strains was measured after 24 h of gentle shaken aerobic growth in BHI broth at 37°C ($n = 5$) compared to the basal concentration of L-lactic acid in BHI medium alone (none). (B) The average growth (OD_{600}) of 4 *S. pneumoniae* strains in *D. pigrum* KPL1914 CFM or in unconditioned BHI broth supplemented with different concentrations of L-lactic acid measured after 19 to 20 h of static aerobic growth at 37°C ($n = 4$). (C) The average growth (OD_{600}) of 2 *S. aureus* strains in *D. pigrum* KPL1914 CFM or in unconditioned BHI broth supplemented with different concentrations of L-lactic acid measured after 19 to 20 h of shaken aerobic growth at 37°C ($n = 4$). In panels A and B, the average pH of the *D. pigrum* CFM was 6.40 (± 0.06). The pH of BHI without lactic acid (0 mM) was adjusted to match the pH of the CFM, to control for any effect of pH alone. Average levels of growth of *S. pneumoniae* in CFM and 11 mM L-lactic acid were analyzed independently for each individual strain using a Wilcoxon rank sum test. Dark bars represent medians, lower and upper hinges correspond to the first and third quartiles, and outlier points are displayed individually, except in panel A, where dots for all individual sample values are represented. *, none of the *S. pneumoniae* or *S. aureus* strains displayed growth in 55 mM L-lactate.

compound(s) toxic/inhibitory to *S. pneumoniae* by either *D. pigrum* or *C. pseudodiphtheriticum* or both *D. pigrum* and *C. pseudodiphtheriticum* when grown together. (Of note, cocultivation of *D. pigrum* and *C. pseudodiphtheriticum* in liquid BHI medium did not increase the level of L-lactic acid compared to growth of *D. pigrum* alone [Fig. S1].) Along with the *Corynebacterium* species enhancement of *D. pigrum* growth yield (Fig. 2) and the *D. pigrum* inhibition of *S. aureus* growth (Fig. 3), these data indicate that the negative associations of *D. pigrum* with *S. aureus* and *S. pneumoniae* are likely mediated by different molecular mechanisms.

To learn more about the functional capacity and genomic structure of *D. pigrum*, we next turned to genomic analysis, which provided insights into some of the epidemiologic and phenotypic observations presented above.

The genomes of 11 *D. pigrum* strains reveal a small genome consistent with a highly host-adapted bacterium. We analyzed one publicly available genome of *D. pigrum* (ATCC 51524) and sequenced 10 additional strains (see Text S1 in the supplemental material), which were selected to ensure representation of distinct strains (see Materials and Methods). To start, we focused on basic genomic characteristics. The 11 *D. pigrum* strain genomes had an average size of 1.86 Mb (median 1.88 Mb) with 1,693 predicted coding sequences (CDS) (see Tables A and B in Text S1). Approximately 1,200 CDS were core (see Fig. A and B and Table C in Text S1) and exhibited a high degree of nucleotide and amino acid sequence conservation (see Fig. C in Text S1). As shown in Text S1, we further analyzed synteny of two closed genomes (see Fig. D in Text S1) and BLAST ring comparisons (see Fig. E in Text S1) and constructed a core-gene-based phylogeny (see Fig. F in Text S1).

***D. pigrum* is a predicted auxotroph for amino acids, polyamines, and enzymatic cofactors.** The nasal environment is low in and/or lacking in key nutrients such as methionine (84), and the small genome size (1.86 Mb) of *D. pigrum* is consistent with reduced biosynthetic capacity. To gain insight into how *D. pigrum* functions in the nasal

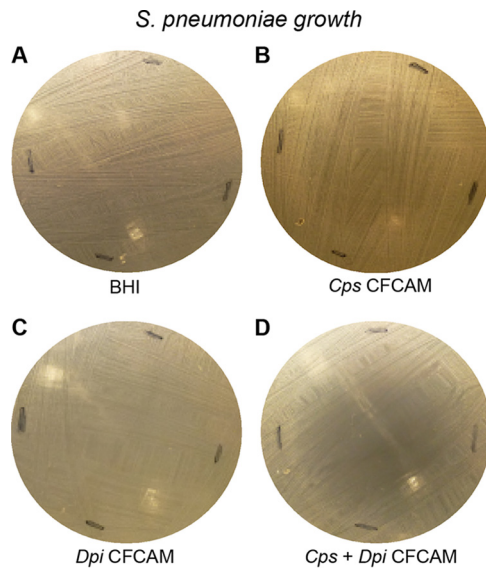


FIG 5 *D. pigrum* and *C. pseudodiphtheriticum* grown together but not *D. pigrum* alone inhibited *S. pneumoniae* in an *in vitro* agar medium-based assay. Representative images are shown of *S. pneumoniae* 603 growth on (A) BHI medium alone or on CFCAM from (B) *C. pseudodiphtheriticum* KPL1989, (C) *D. pigrum* KPL1914, or (D) both *D. pigrum* and *C. pseudodiphtheriticum* grown in a mixed inoculum ($n = 4$). To condition the medium, we cultivated *D. pigrum* and/or *C. pseudodiphtheriticum* on a membrane, which was then removed prior to spreading a lawn of *S. pneumoniae*. For monoculture, 100 μ l of either *D. pigrum* or *C. pseudodiphtheriticum*, resuspended to an $OD_{600} = 0.50$, were inoculated onto the membrane. For mixed coculture, 50 μ l of *D. pigrum* ($OD_{600} = 0.50$) were mixed with 50 μ l of *C. pseudodiphtheriticum* ($OD_{600} = 0.50$) to yield a final volume of 100 μ l for the inoculum, such that each bacterial species was present in the coculture inoculum at half the amount used for the corresponding monoculture inoculum. Images were cropped. Black marks indicate edges where the membrane had been.

environment, we examined all 11 genomes, finding evidence of auxotrophy for some amino acids (e.g., methionine), polyamines (e.g., putrescine and spermidine), and enzymatic cofactors (e.g., biotin) across all strains. In turn, we identified putative degradation pathways (e.g., methionine), transporter pathways (e.g., polyamines and biotin), and salvage pathways (e.g., folate), suggesting that *D. pigrum* acquires some required nutrients exogenously. Section I in Text S2 contains additional details plus predictions of acquisition of metal cofactors. The auxotrophy predictions may be incomplete, since we were unable to grow *D. pigrum* in a chemically defined medium with all 20 amino acids that was putatively replete on the basis of these predictions. Apparent auxotrophy for a number of required nutrients indicates that these must be available either from the host or from neighboring microbes in human nasal passages, e.g., possibly from nasal *Corynebacterium* species.

Whole-genome sequencing indicates that *D. pigrum* metabolizes carbohydrates to lactic acid via homofermentation. *D. pigrum* produced lactate during *in vitro* cultivation (Fig. 4A). Lactic acid bacteria mainly perform either homofermentation or heterofermentation of carbohydrates (85). Therefore, we examined the genomic capacity of *D. pigrum* for carbohydrate metabolism (see section II in Text S2). *D. pigrum* genomes lacked genes required for a complete tricarboxylic acid cycle, which is consistent with fermentation. Moreover, we identified genes encoding a complete glycolytic pathway in all 11 strains that are consistent with homofermentation. All 11 strains harbored a predicted L-lactate dehydrogenase (EC 1.1.1.27) which catalyzes the reduction of pyruvate to lactate, regenerating NAD^+ for glycolysis (GAPDH [glyceraldehyde-3-phosphate dehydrogenase] step), consistent with homofermentation to L-lactate as the main product of glycolysis.

The accessory genome of 11 *D. pigrum* strains contains a diversity of biosynthetic gene clusters predicted to encode antibiotics. Lactic acid production alone appears insufficient to account for the negative *in vitro* associations of *D. pigrum* with

S. aureus and with *S. pneumoniae* (Fig. 4). To delve further into the genetic capacity of *D. pigrum* for possible mechanisms of inhibition, we explored the accessory genome of the 11 sequenced strains. Consistent with a prior report (60), *D. pigrum* appears to be broadly susceptible to antibiotics (see section III in Text S2). What emerged in our analysis was a diversity of biosynthetic gene clusters (BGCs) (see Table A and Fig. A in Text S2), including a diversity of BGCs predicted to encode candidate antibiotics. Strikingly, although 10 of 10 strains tested displayed inhibition of *S. aureus* growth *in vitro* (Fig. 3), there was no single BGC common to all 10 strains that might encode a compound with antibiotic activity. On the basis of these data, we hypothesize that *D. pigrum* uses a diverse repertoire of BGCs to produce bioactive molecules that play key roles in interspecies interactions with its microbial neighbors, e.g., for niche competition, and potentially with its host. This points to a new direction for future research on the functions that underlie the positive associations of *D. pigrum* in human nasal microbiota with health and highlights the need to develop a system for genetic engineering of *D. pigrum*.

DISCUSSION

D. pigrum was shown to be associated with health in multiple genus-level compositional studies of human URT/nasal passage microbiota. In nasal passage microbiota data sets, we identified positive associations of *D. pigrum* with specific species of *Corynebacterium* in adults and children and a negative association of *D. pigrum* with *S. aureus* in adults (Fig. 1). We observed phenotypic support for these associations. First, unilateral cooperation from three common nasal *Corynebacterium* species enhanced *D. pigrum* growth yields (Fig. 2). Second, *D. pigrum* inhibited *S. aureus* (Fig. 3). Our genomic analysis revealed auxotrophies consistent with *D. pigrum* reliance on cocolonizing microbes and/or the human host for key nutrients. Genomic analysis also showed an aerotolerant anaerobe that performs homofermentation to lactate. However, *D. pigrum* lactate production (Fig. 4A) was insufficient to inhibit either *S. pneumoniae* (Fig. 4B) or *S. aureus* (Fig. 4C) and therefore is not the sole contributor to negative associations with *S. pneumoniae* and *S. aureus* *in vivo*. Consistent with the reports of a negative association between *D. pigrum* (usually in conjunction with *Corynebacterium*) and *S. pneumoniae*, we observed that cocultivation of *D. pigrum* and *C. pseudodiphtheriticum* produced a diffusible activity that robustly inhibited *S. pneumoniae* (Fig. 5; see also Fig. S2 in the supplemental material) whereas monoculture of either did not. Finally, we uncovered a surprisingly diverse repertoire of BGCs in 11 *D. pigrum* strains, revealing potential mechanisms for niche competition that were previously unrecognized. These data mark a significant advance in the study of *D. pigrum* and set the stage for future research on molecular mechanisms.

The *in vitro* interactions of *D. pigrum* with *S. aureus* and with *S. pneumoniae* support inferences from composition-level microbiota data of competition between *D. pigrum* and each pathobiont. However, these interactions differed *in vitro*. *D. pigrum* alone inhibited *S. aureus*, but *D. pigrum* plus *C. pseudodiphtheriticum*, together, robustly inhibited *S. pneumoniae*. These results point to a more complex set of interactions among these specific bacterial members of the human nasal microbiota which likely exists in the context of a network of both microbe-microbe and microbe-host interactions. To date, mechanisms for only a few such interactions have been described. For example, a *C. accolens* triacylglycerol lipase (LipS1) releases antipneumococcal free fatty acids from model host surface triacylglycerols *in vitro*, pointing to habitat modification as a possible contributor to *S. pneumoniae* colonization resistance (33).

Multiple mechanisms could result in *D. pigrum* inhibition of *S. aureus* *in vitro*, including nutrient competition and excretion of a toxic primary metabolite or of an anti-*S. aureus* secondary metabolite (i.e., an antibiotic). Initial bioassay-guided fractionation approaches failed to identify such a mechanism. However, the data showing the existence of diverse repertoires of BGCs among the 11 *D. pigrum* strains are intriguing because they include predicted bacteriocins, including lanthipeptides. For example, 4

of the 11 strains harbored putative type II lanthipeptide biosynthetic gene clusters. These clusters are characterized by the presence of the LanM enzyme, containing both dehydration and cyclization domains needed for lanthipeptide biosynthesis (86). Alignment of these enzymes with the enterococcal cytolysin LanM revealed conserved catalytic residues in both domains (87). Cleavage of the leader portion of the lanthipeptide is necessary to produce an active compound, and the presence of peptidases and transporters within these BGCs suggests that these *D. pigrum* strains might secrete an active lanthipeptide, which could play a role in niche competition with other microbes. Additionally, 8 of the 11 *D. pigrum* genomes examined contain putative bacteriocins, or bactericidal proteins and peptides. Intriguingly, the *D. pigrum* strains exhibiting the strongest inhibition of *S. aureus* (CDC4709-98, CDC39-95, and KPL1914) (Fig. 3) were the only strains that contained both a lanthipeptide BGC and a bacteriocin, further indicating that *D. pigrum* may employ multiple mechanisms to inhibit *S. aureus* growth. Also, if both are required for the *in vitro* inhibition, this might explain the negative results from bioassay-guided fractionation. Mechanisms are coming to light that account for how other nasal bacteria interact with *S. aureus*. For example, commensal *Corynebacterium* species excrete a yet-to-be-identified substance that inhibits *S. aureus* autoinducing peptides blocking *agr* quorum sensing (QS), and shifting *S. aureus* toward a commensal phenotype (88). Also, the yet-to-be-identified mechanism of *C. pseudodiphtheriticum* contact-dependent inhibition of *S. aureus* is mediated through phenol-soluble modulins, the expression of which increases during activation of *agr* QS (89). Within broader *Staphylococcus-Corynebacterium* interactions, *C. propinquum* outcompetes coagulase-negative *Staphylococcus*, but not *S. aureus*, for iron *in vitro* using the siderophore dehydroxynocardamine, the genes for which are transcribed *in vivo* in human nostrils (90). Interphylum *Actinobacteria-Firmicutes* interactions also occur between *Cutibacterium acnes* and *Staphylococcus* species (reviewed in reference 14). For example, some strains of *C. acnes* produce an antistaphylococcus thiopeptide, cutimycin, *in vivo* and the presence of the cutimycin BGC is correlated with microbiota composition at the level of the individual human hair follicle (91). Of note, *Actinobacteria* competition with coagulase-negative *Staphylococcus* species could also have network-mediated (indirect) effects on *S. aureus* via the well-known competition among *Staphylococcus* species (reviewed in reference 92), which can be mediated by, e.g., antibiotic production (15–17, 19), interference with *S. aureus agr* QS (18, 20, 93, 94), or extracellular protease activity (95), among other means (14). Further rounding out the emerging complexity of microbe-microbe interactions in nasal microbiota, multiple strains of *Staphylococcus*, particularly *S. epidermidis*, inhibit the *in vitro* growth of other nasal and skin bacteria, including *D. pigrum*, via yet-to-be-identified mechanisms (16). The evidence described above points to a wealth of opportunity to use human nasal microbiota as a model system to learn how bacteria use competition to shape their community.

Direct cooperation could contribute to the observed positive associations between bacterial species in epidemiological microbiome studies. Conditioning medium with any of the three nasal *Corynebacterium* species positively associated with *D. pigrum in vivo* in human nasal microbiota (Fig. 1) enhanced the growth yield of some *D. pigrum* strains (Fig. 2). This is possibly accounted for by excretion of a limiting nutrient or by removal of a toxic medium component. The genomic predictions of auxotrophy might favor nasal *Corynebacterium* species providing cooperation to *D. pigrum* by excretion of a limiting nutrient. Indeed, mass spectrometry indicated that a number of nutrients are limiting in the nose (84).

There were several limitations of our study. First, we analyzed the genomes of 11 strains that were primarily isolated in the setting of disease. It is unclear whether these strains were contaminants or pathogenic contributors (60). However, *D. pigrum* strains are infrequently associated with disease (61–68). These 11 *D. pigrum* strains did not appear to encode potential virulence factors (see section III in Text S2 in the supplemental material), which is consistent with *D. pigrum* acting primarily as a mutualistic species of humans. Second, the ongoing search for a fully defined chemical medium

permissive for *D. pigrum* growth precluded experimental verification of predicted auxotrophies and further investigation of how the presence of nasal *Corynebacterium* enhances *D. pigrum* growth yields. Third, the *D. pigrum* anti-*S. aureus* factor has eluded purification and identification efforts with standard chemistry approaches and *D. pigrum* is not yet genetically tractable, limiting the use of genetic approaches to identify it. Fourth, to date, there has been no animal model for nasal colonization with *D. pigrum* and *Corynebacterium* species, which stymies direct *in vivo* testing of the hypothesis of pathobiont inhibition and points to another area of need within the nasal microbiome field.

In summary, we validated *in vivo* associations from human bacterial microbiota studies with functional assays that support the hypothesis that *D. pigrum* is a mutualist with respect to its human host, rather than a purely commensal bacterium. Further, the data from these phenotypic interactions support the idea of a role for microbe-microbe interactions in shaping the composition of human nasal microbiota and, thus, the possibility of developing microbe-targeted interventions to reshape community composition. The next step will be to identify the molecular mechanisms of those interactions and to assess their role in the human host. Such work could establish the premise for future studies to investigate the therapeutic potential of *D. pigrum* as a topical nasal probiotic for use in patients with recurrent infections with *S. pneumoniae*, possibly in conjunction with a nasal *Corynebacterium* species, or with *S. aureus*, in conjunction with established *S. aureus* decolonization techniques (96).

MATERIALS AND METHODS

Species-level reanalysis of a pediatric nostril microbiota data set. Laufer et al. analyzed nostril swabs collected from 108 children ages 6 to 78 months (26). Of these, 44% were culture positive for *S. pneumoniae* and 23% were diagnosed with otitis media. 16S rRNA gene V1-V2 sequences were generated using Roche/454 with primers 27F and 338R. We obtained 184,685 sequences from the authors, of which 94% included sequence matching primer 338R and 1% included sequence matching primer 27F. We performed demultiplexing in QIIME (97) (split_libraries.py), filtering reads for those ≥ 250 bp in length, those with a quality score of ≥ 30 , and those with barcode type hamming_8. Then, we eliminated sequences from samples for which there were no metadata ($n = 108$ for metadata), leaving 120,963 sequences on which we performed *de novo* chimera removal in QIIME (USEARCH 6.1) (98, 99), yielding 120,274 16S rRNA V1-V2 sequences. We then aligned the 120,274 chimera-cleaned reads in QIIME (PyNASt) (100), using eHOMDv15.04 (41) as a reference database, and trimmed the reads using “o-trim-uninformative-columns-from-alignment” and “o-smart-trim” scripts (101). A total of 116,620 reads (97% of the chimera-cleaned reads) were recovered after the alignment and trimming steps. After these initial cleaning steps, we retained only the 99 samples with more than 250 reads. We analyzed these data set of 99 samples with a total of 114,909 reads using MED (101) with minimum substantive abundance of an oligotype (-M) equal to 4 and maximum variation allowed in each node (-V) equal to 6 nucleotides (nt), which equals 1.6% of the 379-nucleotide length of the trimmed alignment. Of the 114,909 sequences, 82.8% (95,164) passed the -M and -V filtering and are represented in the MED output. Oligotypes were assigned taxonomy in R with the `data2::assignTaxonomy()` function (an implementation of the naive Bayesian RDP classifier algorithm with a kmer size of 8 and a bootstrap value of 100) (102, 103) using the eHOMDv15.1 V1-V3 Training Set (version 1) (41) and a bootstrap value of 70. We then collapsed oligotypes within the same species/supraspecies, yielding the data shown in Table S2 in the supplemental material.

Microbiota community comparison (Fig. 1). The pediatric 16S rRNA gene V1-V2 data set analyzed at the species level (Table S2) and the HMP adult 16S rRNA gene V1-V3 data set previously analyzed at the species level (see Table S7 in reference 41) were used as input for the ANCOM, including all identified taxa (i.e., we did not remove taxa with low relative abundance). ANCOM (version 1.1.3) was performed using the presence or absence of *D. pigrum*, on the basis of the 16S rRNA gene sequencing data, as group definer. ANCOM default parameters were used (sig = 0.05, tau = 0.02, theta = 0.1, repeated = FALSE [i.e., Kruskal-Wallis test]), except that we performed a correction for multiple comparisons (multcorr = 2) instead of using the default no correction (multcorr = 3) (83). The Log relative abundance values for the taxa identified as statistically significant (sig = 0.05) are represented in Fig. 1 and are also available in Table S1.

Cultivation from frozen stocks. Bacterial strains (see Table A in Text S1 in the supplemental material; see also Table S3) were cultivated as described here unless stated otherwise. Across the various methods, strains were grown at 37°C with 5% CO₂ unless otherwise noted. *D. pigrum* strains were cultivated from frozen stocks on BBL Columbia colistin-nalidixic acid (CNA) agar with 5% sheep blood (BD Diagnostics) for 2 days. *Corynebacterium* species were cultivated from frozen stocks on BHI agar (*C. pseudodiphtheriticum* and *C. propinquum*) or on BHI agar supplemented with 1% Tween 80 (*C. accolens*) for 1 day. The resuspensions described below were made by harvesting colonies from agar medium and resuspending in 1× phosphate-buffered saline (PBS). Of note, we primarily use agar medium because in our experience *D. pigrum* exhibits more consistent growth on agar medium than in liquid medium.

Likewise, growth on a semisolid surface is likely to better represent growth on nasal surfaces than would growth under the well-mixed conditions of shaking liquid medium.

Preconditioning growth yield assays (Fig. 2). To assess the growth yield of *D. pigrum* on a polycarbonate membrane atop media conditioned by *Corynebacterium* spp., each *Corynebacterium* strain was resuspended from growth on agar medium to an optical density at 600 nm (OD_{600}) of 0.50 in $1 \times$ PBS. Then, 100 μ l volumes of each resuspension were individually spread onto a 0.2- μ m-pore-size, 47-mm-diameter polycarbonate membrane (EMD Millipore, Billerica, MA) atop 20 ml of either BHI agar for *C. pseudodiphtheriticum* and *C. propinquum* or BHI agar supplemented with triolein (BHIT) (CAS catalog no. 122-32-7, Acros) spread atop the agar medium, as previously described (33), for *C. accolens*. After 2 days of growth, the membranes with *Corynebacterium* cells were removed, leaving CFCAM. On each plate of CFCAM, we placed a new membrane onto which we spread 100 μ l of *D. pigrum* cells that had been resuspended to an OD_{600} of 0.50 in $1 \times$ PBS. After 2 days, the membranes with *D. pigrum* were removed, placed in 3 ml $1 \times$ PBS, and subjected to vortex mixing for 1 min to resuspend cells. Resuspensions were diluted 1:10 six times, dilutions were inoculated onto BBL CNA agar with 5% sheep blood, and CFU were enumerated after 2 to 3 days of growth. To assess the growth yield of *C. pseudodiphtheriticum* on a polycarbonate membrane atop media conditioned by *D. pigrum*, strains KPL1914 and CDC4709-98 were grown for 2 days as described above. *C. pseudodiphtheriticum* KPL1989 growth yield was then measured as described above.

Growth of *D. pigrum* directly on BHI agar medium supplemented with triolein and conditioned by growth of nasal *Corynebacterium* species (Table 1). Onto BHI agar supplemented with 200 U/ml of bovine liver catalase (C40-500MG, Sigma) (BHIC), we spread 50 μ l of 100 mg/ml of triolein (BHICT). We then spread 50 μ l of a resuspension (OD_{600} of 0.50) of each *Corynebacterium* strain onto a 0.2- μ m-pore-size, 47-mm-diameter polycarbonate membrane placed atop 10 ml of BHICT agar in a 100-mm-by-15-mm petri dish. After 2 days, we removed each membrane with *Corynebacterium* cells, leaving CFCAM. Using a sterile cotton swab, we then spread a lawn of either *D. pigrum* (from cells resuspended to an OD_{600} of 0.50 in $1 \times$ PBS) or *S. pneumoniae* (taken directly from agar medium) onto the CFCAM. Each lawn was then grown for 1 to 2 days before documentation of growth or inhibition of growth was performed with digital photography.

Oleic acid disc diffusion assay (Table 2). A lawn of *D. pigrum* or *S. pneumoniae* was spread onto 10 ml of BHIC agar using a sterile cotton swab as described above. Oleic acid (Sigma-Aldrich) was dissolved to reach final concentrations of 2 mg/ml, 5 mg/ml, and 10 mg/ml in ethanol, and then we added 10 μ l of each to separate, sterile 0.2- μ m-pore-size, 6-mm-diameter filter discs (Whatman), with 10 μ l of ethanol alone added to a disc as a control. After the solvent was allowed to evaporate, filter discs were placed on the bacterial lawns, which were then allowed to grow for 1 day before measurement of zones of inhibition and photography were performed.

Growth of *D. pigrum* directly on versus atop a membrane on oleic acid-coated agar medium (Table 3). Oleic acid was dissolved in 100% ethanol to a concentration of 5 mg/ml and then further diluted 10-fold 5 times in ethanol. For each dilution, 100 μ l was spread on a separate plate of BHI agar medium. Next, 10 μ l of *D. pigrum* KPL1914 and CDC4709-98, each resuspended to an $OD_{600} = 0.3$, were inoculated both directly onto the oleic acid-coated agar medium and atop of a 0.2- μ m-pore-size, 47-mm-diameter polycarbonate membrane (EMD Millipore, Billerica, MA) on the same plate. After the plates had been maintained for 2 days at 37°C, we assessed and photographed the growth. In addition, for each dilution and strain, one spot on the membrane was resuspended in PBS to assess CFU counts after serial dilutions and plating on blood agar plates (see above).

***D. pigrum*-*S. aureus* side-by-side coculture assays (Fig. 3).** *D. pigrum* cells were grown from frozen stocks as described above. *S. aureus* JE2 was grown overnight on BBL Columbia CNA agar with 5% sheep blood. Bacterial cells were harvested with sterile cotton swabs and resuspended in sterile $1 \times$ PBS to a minimal OD_{600} of 0.3 for *D. pigrum* and 0.1 for *S. aureus*. Next, 5- μ l drops were individually inoculated on BHI agar medium and incubated for 2 days for *D. pigrum* and 1 day for *S. aureus*. Then, 5- μ l drops of resuspended bacteria to be screened for inhibition were inoculated at different distances from the pregrown bacteria. Inhibition was assessed daily and photographically documented.

Measurement of L-lactic acid concentration (Fig. 4A). *S. pneumoniae*, *S. aureus*, *C. pseudodiphtheriticum*, and *D. pigrum* cells were grown from frozen stocks as described above. Cells were then harvested with a sterile cotton swab, resuspended to an OD_{600} of 0.50 in $1 \times$ PBS, and inoculated at 1:25 into BHI broth for overnight growth with gently shaking (~50 to ~60 rpm) at 37°C under atmospheric conditions. For mixed subcultures, i.e., *C. pseudodiphtheriticum* and *D. pigrum*, a 1:1 mixture was inoculated at 1:25 into fresh BHI broth. The overnight culture was then inoculated at 1:25 into fresh BHI broth and grown for 24 h at 37°C prior to measurement of the lactic acid concentration (mmol/liter) using a D-lactic acid/L-lactic acid kit (catalog no. 11112821035, R-Biopharm AG) per the instructions of the manufacturer and BHI as a negative control.

Growth of *S. aureus* and *S. pneumoniae* in *D. pigrum* cell-free conditioned liquid medium (CFCM in Fig. 4B and C). After growth in BHI, as described for L-lactic acid measurement, the *D. pigrum* KPL1914 cells were removed with a 0.22- μ m-pore-size sterile filter, yielding cell-free conditioned medium (CFCM). Each of *S. aureus* strains Newman and JE2 and *S. pneumoniae* strains TIGR4, DBL5, 603, and WU2 was grown on BBL Columbia CNA agar with 5% sheep blood for 1 day, harvested with a sterile cotton swab, resuspended to an OD_{600} of 0.30 in $1 \times$ PBS, inoculated at 1:100 into both *D. pigrum* CFCM and BHI broth, and grown for 19 to 20 h at 37°C in shaking (*S. aureus*; 50 rpm) or static (*S. pneumoniae*) culture under atmospheric conditions. Growth yield was quantified as OD_{600} absorbance.

Growth of *S. aureus* and *S. pneumoniae* in BHI broth supplemented with L-lactic acid (see lactic acid data in Fig. 4B and C). Strains of *S. aureus* and *S. pneumoniae* were grown and harvested as

described above for inoculation. BHI broth, supplemented with L-lactic acid (CAS no. 79-33-4; Fisher BioReagents) at various concentrations from 11 mM to 55 mM, was sterilized through a 0.22- μ m-pore-size filter. After inoculation of each strain separately into BHI broth with L-lactic acid, cultures were grown as described above for growth in CFCM. Growth yield was quantified as OD₆₀₀ absorbance.

Growth assay for *S. pneumoniae* on BHI agar medium conditioned by monoculture versus coculture of *D. pigrum* and/or *C. pseudodiphtheriticum* (Fig. 5; see also Fig. S2 in the supplemental material). *D. pigrum* and *C. pseudodiphtheriticum* strains were grown from freezer stocks as described above. Cells were harvested with sterile cotton swabs and resuspended in sterile PBS to an OD₆₀₀ of 0.5. We then spotted 100 μ l of 1:1 mixed resuspension on a polycarbonate membrane (see above) on BHI agar medium containing 400 U/ml bovine liver catalase. After 2 days of growth, the polycarbonate membrane with *D. pigrum* and/or *C. pseudodiphtheriticum* was removed from each plate, leaving CFCAM. *S. pneumoniae* 603 (104) was grown overnight on BBL Columbia CNA agar with 5% sheep blood as described above, and, using a sterile cotton swab, a lawn was streaked onto the CFCAM and allowed to grow for 24 h. Growth/inhibition was assessed daily and photographically recorded. Imaging was difficult due to the transparency of *S. pneumoniae* lawns.

Statistical analyses. R version 3.6.2 was used for statistical analysis and data visualization. The Wilcoxon rank sum test (equivalent to the Mann-Whitney test) was performed using `wilcox.test()` with `paired = FALSE`, `alternative = "two.sided"`.

Ethics approval and consent to participate. We isolated *D. pigrum* KPL1914 and *C. pseudodiphtheriticum* KPL1989 from the nostril of an adult as part of a protocol to study the bacterial microbiota of the nostrils of healthy adults that was initially approved by the Harvard Medical School Committee on Human Studies (105) and subsequently approved by the Forsyth Institute Institutional Review Board.

Data availability. We declare that all data that support the findings of this study are available within the paper (and its supplemental material); from publicly available repositories, i.e., GenBank (BioProject accession numbers [PRJNA379818](#) and [PRJNA379966](#)); or from the corresponding authors upon reasonable request. All computer code for published tools used in this work is referenced in Materials and Methods; custom-made code (i.e., loop code) is described in Materials and Methods. Further details are available from the corresponding authors on reasonable request.

SUPPLEMENTAL MATERIAL

Supplemental material is available online only.

TEXT S1, PDF file, 2.5 MB.

TEXT S2, PDF file, 0.8 MB.

FIG S1, PDF file, 0.04 MB.

FIG S2, PDF file, 0.1 MB.

TABLE S1, XLSX file, 0.02 MB.

TABLE S2, XLSX file, 0.1 MB.

TABLE S3, DOCX file, 0.03 MB.

ACKNOWLEDGMENTS

We thank Richard R. Facklam and Lynn Shewmaker for providing strains; Joshua Metlay for providing data; Markus Hilty and Stephany Flores Ramos for manuscript edits; and Markus Hilty, Lindsey Bomar, Srikanth Mairpady Shambat, Annelies Zinker-nagel, and members of the Lemon lab for helpful input and discussions.

This work was supported by the National Institutes of Health through the National Institute of General Medical Sciences (grant R01 GM117174 to K.P.L.) and the National Institute of Deafness and other Communication Disorders (grant R01 DC013554 to M.M.P.); by the Swiss National Science Foundation and Swiss Foundation for Grants in Biology and Medicine (grant P3SMP3_155315 to S.D.B.); by the Novartis Foundation for Medical-Biological Research (grant 16B065 to S.D.B.); and by the Promedica Foundation (grant 1449/M to S.D.B.). The funders had no role in the preparation of the manuscript or the decision to publish.

Our contributions were as follows: conceptualization, S.D.B., M.M.P., and K.P.L.; methodology, S.D.B., S.M.E., and M.T.H.; investigation, S.D.B., S.M.E., I.F.E., and Y.K.; interpretation of data, S.D.B., S.M.E., M.M.P., I.F.E., M.T.H., Y.K., and K.P.L.; visualization, S.D.B., S.M.E., and I.F.E.; writing of the original draft, S.D.B., S.M.E., and K.P.L.; editing and review, S.D.B., M.M.P., S.M.E., I.F.E., and K.P.L.; supervision, S.D.B. and K.P.L.; funding acquisition, S.D.B., M.M.P., and K.P.L.

Consent for publication is not applicable.

We declare no competing interests.

REFERENCES

- Bogaert D, De Groot R, Hermans PW. 2004. *Streptococcus pneumoniae* colonisation: the key to pneumococcal disease. *Lancet Infect Dis* 4:144–154. [https://doi.org/10.1016/S1473-3099\(04\)00938-7](https://doi.org/10.1016/S1473-3099(04)00938-7).
- von Eiff C, Becker K, Machka K, Stammer H, Peters G. 2001. Nasal carriage as a source of *Staphylococcus aureus* bacteremia. *N Engl J Med* 344:11–16. <https://doi.org/10.1056/NEJM200101043440102>.
- Wertheim HF, Vos MC, Ott A, van Belkum A, Voss A, Kluytmans JA, van Keulen PH, Vandenbroucke-Grauls CM, Meester MH, Verbrugh HA. 2004. Risk and outcome of nosocomial *Staphylococcus aureus* bacteraemia in nasal carriers versus non-carriers. *Lancet* 364:703–705. [https://doi.org/10.1016/S0140-6736\(04\)16897-9](https://doi.org/10.1016/S0140-6736(04)16897-9).
- Kluytmans J, van Belkum A, Verbrugh H. 1997. Nasal carriage of *Staphylococcus aureus*: epidemiology, underlying mechanisms, and associated risks. *Clin Microbiol Rev* 10:505–520. <https://doi.org/10.1128/CMR.10.3.505-520.1997>.
- Young BC, Wu CH, Gordon NC, Cole K, Price JR, Liu E, Sheppard AE, Perera S, Charlesworth J, Golubchik T, Iqbal Z, Bowden R, Massey RC, Paul J, Crook DW, Peto TE, Walker AS, Llewelyn MJ, Wyllie DH, Wilson DJ. 2017. Severe infections emerge from commensal bacteria by adaptive evolution. *Elife* 6:e30637. <https://doi.org/10.7554/eLife.30637>.
- Bode LG, Kluytmans JA, Wertheim HF, Bogaers D, Vandenbroucke-Grauls CM, Roosendaal R, Troelstra A, Box AT, Voss A, van der Tweel I, van Belkum A, Verbrugh HA, Vos MC. 2010. Preventing surgical-site infections in nasal carriers of *Staphylococcus aureus*. *N Engl J Med* 362:9–17. <https://doi.org/10.1056/NEJMoa0808939>.
- Lexau CA, Lynfield R, Danila R, Pilishvili T, Facklam R, Farley MM, Harrison LH, Schaffner W, Reingold A, Bennett NM, Hadler J, Cieslak PR, Whitney CG, Active Bacterial Core Surveillance Team. 2005. Changing epidemiology of invasive pneumococcal disease among older adults in the era of pediatric pneumococcal conjugate vaccine. *JAMA* 294:2043–2051. <https://doi.org/10.1001/jama.294.16.2043>.
- Wahl B, O'Brien KL, Greenbaum A, Majumder A, Liu L, Chu Y, Luksic I, Nair H, McAllister DA, Campbell H, Rudan I, Black R, Knoll MD. 2018. Burden of *Streptococcus pneumoniae* and *Haemophilus influenzae* type b disease in children in the era of conjugate vaccines: global, regional, and national estimates for 2000–15. *Lancet Glob Health* 6:e744–e757. [https://doi.org/10.1016/S2214-109X\(18\)30247-X](https://doi.org/10.1016/S2214-109X(18)30247-X).
- GBD 2016 Lower Respiratory Infections Collaborators. 2018. Estimates of the global, regional, and national morbidity, mortality, and aetiologies of lower respiratory infections in 195 countries, 1990–2016: a systematic analysis for the Global Burden of Disease Study 2016. *Lancet Infect Dis* 18:1191–1210. [https://doi.org/10.1016/S1473-3099\(18\)30310-4](https://doi.org/10.1016/S1473-3099(18)30310-4).
- Tong SY, Davis JS, Eichenberger E, Holland TL, Fowler VG, Jr. 2015. *Staphylococcus aureus* infections: epidemiology, pathophysiology, clinical manifestations, and management. *Clin Microbiol Rev* 28:603–661. <https://doi.org/10.1128/CMR.00134-14>.
- Turner NA, Sharma-Kuinkel BK, Maskarinec SA, Eichenberger EM, Shah PP, Carugati M, Holland TL, Fowler VG, Jr. 2019. Methicillin-resistant *Staphylococcus aureus*: an overview of basic and clinical research. *Nat Rev Microbiol* 17:203–218. <https://doi.org/10.1038/s41579-018-0147-4>.
- WHO. 2012. Pneumococcal vaccines WHO position paper - 2012 - recommendations. *Vaccine* 30:4717–4718. <https://doi.org/10.1016/j.vaccine.2012.04.093>.
- Schulfer A, Blaser MJ. 2015. Risks of antibiotic exposures early in life on the developing microbiome. *PLoS Pathog* 11:e1004903. <https://doi.org/10.1371/journal.ppat.1004903>.
- Brugger SD, Bomar L, Lemon KP. 2016. Commensal-pathogen interactions along the human nasal passages. *PLoS Pathog* 12:e1005633. <https://doi.org/10.1371/journal.ppat.1005633>.
- Zipperer A, Konnerth MC, Laux C, Berscheid A, Janek D, Weidenmaier C, Burian M, Schilling NA, Slavetinsky C, Marschal M, Willmann M, Kalbacher H, Schittek B, Brotz-Oesterhelt H, Grond S, Peschel A, Krismer B. 2016. Human commensals producing a novel antibiotic impair pathogen colonization. *Nature* 535:511–516. <https://doi.org/10.1038/nature18634>.
- Janek D, Zipperer A, Kulik A, Krismer B, Peschel A. 2016. High frequency and diversity of antimicrobial activities produced by nasal *staphylococcus* strains against bacterial competitors. *PLoS Pathog* 12:e1005812. <https://doi.org/10.1371/journal.ppat.1005812>.
- Nakatsuji T, Chen TH, Narala S, Chun KA, Two AM, Yun T, Shafiq F, Kotol PF, Bouslimani A, Melnik AV, Latif H, Kim JN, Lockhart A, Artis K, David G, Taylor P, Streib J, Dorrestein PC, Grier A, Gill SR, Zengler K, Hata TR, Leung DY, Gallo RL. 2017. Antimicrobials from human skin commensal bacteria protect against *Staphylococcus aureus* and are deficient in atopic dermatitis. *Sci Transl Med* 9:eaah4680. <https://doi.org/10.1126/scitranslmed.aah4680>.
- Paharik AE, Parlet CP, Chung N, Todd DA, Rodriguez EI, Van Dyke MJ, Cech NB, Horswill AR. 2017. Coagulase-negative staphylococcal strain prevents *staphylococcus aureus* colonization and skin infection by blocking quorum sensing. *Cell Host Microbe* 22:746–756.e5. <https://doi.org/10.1016/j.chom.2017.11.001>.
- O'Sullivan JN, Rea MC, O'Connor PM, Hill C, Ross RP. 2019. Human skin microbiota is a rich source of bacteriocin-producing staphylococci that kill human pathogens. *FEMS Microbiol Ecol* 95:fy241. <https://doi.org/10.1093/femsec/fy241>.
- Williams MR, Costa SK, Zaramela LS, Khalil S, Todd DA, Winter HL, Sanford JA, O'Neill AM, Liggins MC, Nakatsuji T, Cech NB, Cheung AL, Zengler K, Horswill AR, Gallo RL. 2019. Quorum sensing between bacterial species on the skin protects against epidermal injury in atopic dermatitis. *Sci Transl Med* 11:eaat8329. <https://doi.org/10.1126/scitranslmed.aat8329>.
- Piewngam P, Zheng Y, Nguyen TH, Dickey SW, Joo HS, Villaruz AE, Glose KA, Fisher EL, Hunt RL, Li B, Chiou J, Pharkjaksu S, Khongthong S, Cheung GYC, Kiratisin P, Otto M. 2018. Pathogen elimination by probiotic *Bacillus* via signalling interference. *Nature* 562:532–537. <https://doi.org/10.1038/s41586-018-0616-y>.
- Tano K, Hakansson EG, Holm SE, Hellstrom S. 2002. Bacterial interference between pathogens in otitis media and alpha-haemolytic *Streptococci* analysed in an in vitro model. *Acta Otolaryngol* 122:78–85. <https://doi.org/10.1080/00016480252775788>.
- Coleman A, Cervin A. 2019. Probiotics in the treatment of otitis media. The past, the present and the future. *Int J Pediatr Otorhinolaryngol* 116:135–140. <https://doi.org/10.1016/j.ijporl.2018.10.023>.
- Cardenas N, Martin V, Arroyo R, Lopez M, Carrera M, Badiola C, Jimenez E, Rodriguez JM. 2019. Prevention of recurrent acute otitis media in children through the use of *Lactobacillus salivarius* PS7, a target-specific probiotic strain. *Nutrients* 11:376. <https://doi.org/10.3390/nu11020376>.
- Manning J, Dunne EM, Wescombe PA, Hale JD, Mulholland EK, Tagg JR, Robins-Browne RM, Satzke C. 2016. Investigation of *Streptococcus salivarius*-mediated inhibition of pneumococcal adherence to pharyngeal epithelial cells. *BMC Microbiol* 16:225. <https://doi.org/10.1186/s12866-016-0843-z>.
- Laufer AS, Metlay JP, Gent JF, Fennie KP, Kong Y, Pettigrew MM. 2011. Microbial communities of the upper respiratory tract and otitis media in children. *mBio* 2:e00245-10. <https://doi.org/10.1128/mBio.00245-10>.
- Pettigrew MM, Laufer AS, Gent JF, Kong Y, Fennie KP, Metlay JP. 2012. Upper respiratory tract microbial communities, acute otitis media pathogens, and antibiotic use in healthy and sick children. *Appl Environ Microbiol* 78:6262–6270. <https://doi.org/10.1128/AEM.01051-12>.
- Biesbroek G, Bosch AA, Wang X, Keijser BJ, Veenhoven RH, Sanders EA, Bogaert D. 2014. The impact of breastfeeding on nasopharyngeal microbial communities in infants. *Am J Respir Crit Care Med* 190:298–308. <https://doi.org/10.1164/rccm.201401-0073OC>.
- Biesbroek G, Tsvitvadze E, Sanders EA, Montijn R, Veenhoven RH, Keijser BJ, Bogaert D. 2014. Early respiratory microbiota composition determines bacterial succession patterns and respiratory health in children. *Am J Respir Crit Care Med* 190:1283–1292. <https://doi.org/10.1164/rccm.201407-1240OC>.
- Liu CM, Price LB, Hungate BA, Abraham AG, Larsen LA, Christensen K, Stegger M, Skov R, Andersen PS. 2015. *Staphylococcus aureus* and the ecology of the nasal microbiome. *Sci Adv* 1:e1400216. <https://doi.org/10.1126/sciadv.1400216>.
- Teo SM, Mok D, Pham K, Kusel M, Serralha M, Troy N, Holt BJ, Hales BJ, Walker ML, Hollams E, Bochkov YA, Grindie K, Johnston SL, Gern JE, Sly PD, Holt PG, Holt KE, Inouye M. 2015. The infant nasopharyngeal microbiome impacts severity of lower respiratory infection and risk of asthma development. *Cell Host Microbe* 17:704–715. <https://doi.org/10.1016/j.chom.2015.03.008>.
- Bosch A, Levin E, van Houten MA, Hasrat R, Kalkman G, Biesbroek G, de Steenhuijsen Pters WAA, de Groot PCM, Pernet P, Keijser BJF, Sanders EAM, Bogaert D. 2016. Development of upper respiratory tract microbiota in infancy is affected by mode of delivery. *EBioMedicine* 9:336–345. <https://doi.org/10.1016/j.ebiom.2016.05.031>.

33. Bomar L, Brugger SD, Yost BH, Davies SS, Lemon KP. 2016. *Corynebacterium accolens* releases triacylglycerol free fatty acids from human nostril and skin surface triacylglycerols. *mBio* 7:e01725-15. <https://doi.org/10.1128/mBio.01725-15>.
34. Zhang M, Wang R, Liao Y, Buijs MJ, Li J. 2016. Profiling of oral and nasal microbiome in children with cleft palate. *Cleft Palate Craniofac J* 53: 332–338. <https://doi.org/10.1597/14-162>.
35. Salter SJ, Turner C, Watthanaworawit W, de Goffau MC, Wagner J, Parkhill J, Bentley SD, Goldblatt D, Nosten F, Turner P. 2017. A longitudinal study of the infant nasopharyngeal microbiota: the effects of age, illness and antibiotic use in a cohort of South East Asian children. *PLoS Negl Trop Dis* 11:e0005975. <https://doi.org/10.1371/journal.pntd.0005975>.
36. Bosch A, de Steenhuijsen Piters WAA, van Houten MA, Chu M, Biesbroek G, Kool J, Pernet P, de Groot PCM, Eijkemans MJC, Keijser BJJ, Sanders EAM, Bogaert D. 2017. Maturation of the infant respiratory microbiota, environmental drivers, and health consequences. A prospective cohort study. *Am J Respir Crit Care Med* 196:1582–1590. <https://doi.org/10.1164/rccm.201703-0554OC>.
37. Kelly MS, Surette MG, Smieja M, Pernica JM, Rossi L, Luinstra K, Steenhoff AP, Feemster KA, Goldfarb DM, Arscott-Mills T, Boiditswe S, Rulaganayang I, Muthoga C, Gaofwe L, Mazhani T, Rawls JF, Cunningham CK, Shah SS, Seed PC. 2017. The nasopharyngeal microbiota of children with respiratory infections in Botswana. *Pediatr Infect Dis J* 36: e211–e218. <https://doi.org/10.1097/INF.0000000000001607>.
38. Hasegawa K, Linnemann RW, Mansbach JM, Ajami NJ, Espinola JA, Petrosino JF, Piedra PA, Stevenson MD, Sullivan AF, Thompson AD, Camargo CA, Jr. 2017. Nasal airway microbiota profile and severe bronchiolitis in infants: a case-control study. *Pediatr Infect Dis J* 36: 1044–1051. <https://doi.org/10.1097/INF.0000000000001500>.
39. Langevin S, Pichon M, Smith E, Morrison J, Bent Z, Green R, Barker K, Solberg O, Gillet Y, Javouhey E, Lina B, Katze MG, Josset L. 2017. Early nasopharyngeal microbial signature associated with severe influenza in children: a retrospective pilot study. *J Gen Virol* 98:2425–2437. <https://doi.org/10.1099/jgv.0.000920>.
40. Lappan R, Imbrogno G, Sikazwe C, Anderson D, Mok D, Coates H, Vijayasekaran S, Bumbak P, Blyth CC, Jamieson SE, Peacock CS. 2018. A microbiome case-control study of recurrent acute otitis media identified potentially protective bacterial genera. *BMC Microbiol* 18:13. <https://doi.org/10.1186/s12866-018-1154-3>.
41. Escapa IF, Chen T, Huang Y, Gajare P, Dewhurst FE, Lemon KP. 2018. New insights into human nostril microbiome from the expanded human oral microbiome database (eHOMD): a resource for the microbiome of the human aerodigestive tract. *mSystems* 3:e00178-18. <https://doi.org/10.1128/mSystems.00187-18>.
42. Wen Z, Xie G, Zhou Q, Qiu C, Li J, Hu Q, Dai W, Li D, Zheng Y, Wen F. 2018. Distinct nasopharyngeal and oropharyngeal microbiota of children with influenza A virus compared with healthy children. *Biomed Res Int* 2018:6362716. <https://doi.org/10.1155/2018/6362716>.
43. Copeland E, Leonard K, Carney R, Kong J, Forer M, Naidoo Y, Oliver BGG, Seymour JR, Woodcock S, Burke CM, Stow NW. 2018. Chronic rhinosinusitis: potential role of microbial dysbiosis and recommendations for sampling sites. *Front Cell Infect Microbiol* 8:57. <https://doi.org/10.3389/fcimb.2018.00057>.
44. Boelsen LK, Dunne EM, Mika M, Eggers S, Nguyen CD, Ratu FT, Russell FM, Mulholland EK, Hilty M, Satzke C. 2019. The association between pneumococcal vaccination, ethnicity, and the nasopharyngeal microbiota of children in Fiji. *Microbiome* 7:106. <https://doi.org/10.1186/s40168-019-0716-4>.
45. Toivonen L, Hasegawa K, Waris M, Ajami NJ, Petrosino JF, Camargo CA, Jr, Peltola V. 2019. Early nasal microbiota and acute respiratory infections during the first years of life. *Thorax* 74:592–599. <https://doi.org/10.1136/thoraxjnl-2018-212629>.
46. Camelo-Castillo A, Henares D, Brotons P, Galiana A, Rodriguez JC, Mira A, Munoz-Almagro C. 2019. Nasopharyngeal microbiota in children with invasive pneumococcal disease: identification of bacteria with potential disease-promoting and protective effects. *Front Microbiol* 10:11. <https://doi.org/10.3389/fmicb.2019.00011>.
47. Man WH, Clerc M, de Steenhuijsen Piters WAA, van Houten MA, Chu M, Kool J, Keijser BJJ, Sanders EAM, Bogaert D. 2019. Loss of microbial topography between oral and nasopharyngeal microbiota and development of respiratory infections early in life. *Am J Respir Crit Care Med* 200:760–770. <https://doi.org/10.1183/13993003.congress-2019.PA4995>.
48. Man WH, van Houten MA, Merelle ME, Vlieger AM, Chu M, Jansen NJG, Sanders EAM, Bogaert D. 2019. Bacterial and viral respiratory tract microbiota and host characteristics in children with lower respiratory tract infections: a matched case-control study. *Lancet Respir Med* 7:417–426. [https://doi.org/10.1016/S2213-2600\(18\)30449-1](https://doi.org/10.1016/S2213-2600(18)30449-1).
49. Man WH, van Dongen TMA, Venekamp RP, Pluimackers VG, Chu M, van Houten MA, Sanders EAM, Schilder AGM, Bogaert D. 2019. Respiratory microbiota predicts clinical disease course of acute otitis media in children with tympanostomy tubes. *Pediatr Infect Dis J* 38:e116–e125. <https://doi.org/10.1097/INF.0000000000002215>.
50. Gan W, Yang F, Tang Y, Zhou D, Qing D, Hu J, Liu S, Liu F, Meng J. 2019. The difference in nasal bacterial microbiome diversity between chronic rhinosinusitis patients with polyps and a control population. *Int Forum Allergy Rhinol* 9:582–592. <https://doi.org/10.1002/alr.22297>.
51. de Steenhuijsen Piters WAA, Jochems SP, Mitsi E, Rylance J, Pojar S, Nikolaou E, German EL, Holloway M, Carniel BF, Chu M, Arp K, Sanders EAM, Ferreira DM, Bogaert D. 2019. Interaction between the nasal microbiota and *S. pneumoniae* in the context of live-attenuated influenza vaccine. *Nat Commun* 10:2981. <https://doi.org/10.1038/s41467-019-10814-9>.
52. De Boeck I, Wittouck S, Martens K, Claes J, Jorissen M, Steelant B, van den Broek MFL, Seys SF, Hellings PW, Vanderveken OM, Lebeer S. 2019. Anterior nares diversity and pathobionts represent sinus microbiome in chronic rhinosinusitis. *mSphere* 4:e00532-19. <https://doi.org/10.1128/mSphere.00532-19>.
53. Man WH, Scheltema NM, Clerc M, van Houten MA, Nibbelke EE, Achten NB, Arp K, Sanders EAM, Bont LJ, Bogaert D. 2020. Infant respiratory syncytial virus prophylaxis and nasopharyngeal microbiota until 6 years of life: a subanalysis of the MAKI randomised controlled trial. *Lancet Respir Med* S2216–S2600:30170–30479. [https://doi.org/10.1016/S2213-2600\(19\)30470-9](https://doi.org/10.1016/S2213-2600(19)30470-9).
54. Krismer B, Weidenmaier C, Zipperer A, Peschel A. 2017. The commensal lifestyle of *Staphylococcus aureus* and its interactions with the nasal microbiota. *Nat Rev Microbiol* 15:675–687. <https://doi.org/10.1038/nrmicro.2017.104>.
55. Man WH, de Steenhuijsen Piters WA, Bogaert D. 2017. The microbiota of the respiratory tract: gatekeeper to respiratory health. *Nat Rev Microbiol* 15:259–270. <https://doi.org/10.1038/nrmicro.2017.14>.
56. Bomar L, Brugger SD, Lemon KP. 2018. Bacterial microbiota of the nasal passages across the span of human life. *Curr Opin Microbiol* 41:8–14. <https://doi.org/10.1016/j.mib.2017.10.023>.
57. Esposito S, Principi N. 2018. Impact of nasopharyngeal microbiota on the development of respiratory tract diseases. *Eur J Clin Microbiol Infect Dis* 37:1–7. <https://doi.org/10.1007/s10096-017-3076-7>.
58. Aguirre M, Morrison D, Cookson BD, Gay FW, Collins MD. 1993. Phenotypic and phylogenetic characterization of some *Gemella*-like organisms from human infections: description of *Dolosigranulum pigrum* gen. nov., sp. nov. *J Appl Bacteriol* 75:608–612. <https://doi.org/10.1111/j.1365-2672.1993.tb01602.x>.
59. Yan M, Pamp SJ, Fukuyama J, Hwang PH, Cho DY, Holmes S, Relman DA. 2013. Nasal microenvironments and interspecific interactions influence nasal microbiota complexity and *S. aureus* carriage. *Cell Host Microbe* 14:631–640. <https://doi.org/10.1016/j.chom.2013.11.005>.
60. Laclaire L, Facklam R. 2000. Antimicrobial susceptibility and clinical sources of *Dolosigranulum pigrum* cultures. *Antimicrob Agents Chemother* 44: 2001–2003. <https://doi.org/10.1128/aac.44.7.2001-2003.2000>.
61. Hall GS, Gordon S, Schroeder S, Smith K, Anthony K, Procop GW. 2001. Case of synovitis potentially caused by *Dolosigranulum pigrum*. *J Clin Microbiol* 39:1202–1203. <https://doi.org/10.1128/JCM.39.3.1202-1203.2001>.
62. Hoedemaekers A, Schulin T, Tonk B, Melchers WJ, Sturm PD. 2006. Ventilator-associated pneumonia caused by *Dolosigranulum pigrum*. *J Clin Microbiol* 44:3461–3462. <https://doi.org/10.1128/JCM.01050-06>.
63. Lin JC, Hou SJ, Huang LU, Sun JR, Chang WK, Lu JJ. 2006. Acute cholecystitis accompanied by acute pancreatitis potentially caused by *Dolosigranulum pigrum*. *J Clin Microbiol* 44:2298–2299. <https://doi.org/10.1128/JCM.02520-05>.
64. Lecuyer H, Audibert J, Bobigny A, Eckert C, Janniere-Nartey C, Buu-Hoi A, Mainardi JL, Podglajen I. 2007. *Dolosigranulum pigrum* causing nosocomial pneumonia and septicemia. *J Clin Microbiol* 45:3474–3475. <https://doi.org/10.1128/JCM.01373-07>.
65. Johnsen BO, Ronning EJ, Onken A, Figved W, Jenum PA. 2011. *Dolosigranulum pigrum* causing biomaterial-associated arthritis. *APMIS* 119: 85–87. <https://doi.org/10.1111/j.1600-0463.2010.02697.x>.
66. Haas W, Gearinger LS, Hesje CK, Sanfilippo CM, Morris TW. 2012.

- Microbiological etiology and susceptibility of bacterial conjunctivitis isolates from clinical trials with ophthalmic, twice-daily besifloxacin. *Adv Ther* 29:442–455. <https://doi.org/10.1007/s12325-012-0023-y>.
67. Sampo M, Ghazouani O, Cadiou D, Trichet E, Hoffart L, Drancourt M. 2013. *Dolosigranulum pigrum* keratitis: a three-case series. *BMC Ophthalmol* 13:31. <https://doi.org/10.1186/1471-2415-13-31>.
 68. Venkateswaran N, Kalsow CM, Hindman HB. 2014. Phlyctenular keratoconjunctivitis associated with *Dolosigranulum pigrum*. *Ocul Immunol Inflamm* 22:242–245. <https://doi.org/10.3109/09273948.2013.841484>.
 69. Wos-Oxley ML, Plumeier I, von Eiff C, Taudien S, Platzer M, Vilchez-Vargas R, Becker K, Pieper DH. 2010. A poke into the diversity and associations within human anterior nares microbial communities. *ISME J* 4:839–851. <https://doi.org/10.1038/ismej.2010.15>.
 70. Bogaert D, Keijsers B, Huse S, Rossen J, Veenhoven R, van Gils E, Bruin J, Montijn R, Bonten M, Sanders E. 2011. Variability and diversity of nasopharyngeal microbiota in children: a metagenomic analysis. *PLoS One* 6:e17035. <https://doi.org/10.1371/journal.pone.0017035>.
 71. Camarinha-Silva A, Jauregui R, Pieper DH, Wos-Oxley ML. 2012. The temporal dynamics of bacterial communities across human anterior nares. *Environ Microbiol Rep* 4:126–132. <https://doi.org/10.1111/j.1758-2229.2011.00313.x>.
 72. Camarinha-Silva A, Wos-Oxley ML, Jauregui R, Becker K, Pieper DH. 2012. Validating T-RFLP as a sensitive and high-throughput approach to assess bacterial diversity patterns in human anterior nares. *FEMS Microbiol Ecol* 79:98–108. <https://doi.org/10.1111/j.1574-6941.2011.01197.x>.
 73. Sakwinska O, Bastic Schmid V, Berger B, Bruttin A, Keitel K, Lepage M, Moine D, Ngom Bru C, Brussow H, Gervaix A. 2014. Nasopharyngeal microbiota in healthy children and pneumonia patients. *J Clin Microbiol* 52:1590–1594. <https://doi.org/10.1128/JCM.03280-13>.
 74. Peterson SW, Knox NC, Golding GR, Tyler SD, Tyler AD, Mabon P, Embree JE, Fleming F, Fanella S, Van Domselaar G, Mulvey MR, Graham MR. 2016. A study of the infant nasal microbiome development over the first year of life and in relation to their primary adult caregivers using cpn60 universal target (UT) as a phylogenetic marker. *PLoS One* 11:e0152493. <https://doi.org/10.1371/journal.pone.0152493>.
 75. Perez-Losada M, Alamri L, Crandall KA, Freishtat RJ. 2017. Nasopharyngeal microbiome diversity changes over time in children with asthma. *PLoS One* 12:e0170543. <https://doi.org/10.1371/journal.pone.0170543>.
 76. Chonmaitree T, Jennings K, Golovko G, Khanipov K, Pimenova M, Patel JA, McCormick DP, Loeffelholz MJ, Fofanov Y. 2017. Nasopharyngeal microbiota in infants and changes during viral upper respiratory tract infection and acute otitis media. *PLoS One* 12:e0180630. <https://doi.org/10.1371/journal.pone.0180630>.
 77. Luna PN, Hasegawa K, Ajami NJ, Espinola JA, Henke DM, Petrosino JF, Piedra PA, Sullivan AF, Camargo CA, Jr, Shaw CA, Mansbach JM. 2018. The association between anterior nares and nasopharyngeal microbiota in infants hospitalized for bronchiolitis. *Microbiome* 6:2. <https://doi.org/10.1186/s40168-017-0385-0>.
 78. Caputo M, Zoch-Lesniak B, Karch A, Vital M, Meyer F, Klawonn F, Baillet A, Pieper DH, Mikolajczyk RT. 2019. Bacterial community structure and effects of picornavirus infection on the anterior nares microbiome in early childhood. *BMC Microbiol* 19:1. <https://doi.org/10.1186/s12866-018-1372-8>.
 79. Song C, Chorath J, Pak Y, Redjal N. 2019. Use of dipstick assay and rapid PCR-DNA analysis of nasal secretions for diagnosis of bacterial sinusitis in children with chronic cough. *Allergy Rhinol (Providence)* 10:2152656718821281. <https://doi.org/10.1177/2152656718821281>.
 80. Walker RE, Walker CG, Camargo CA, Jr, Bartley J, Flint D, Thompson JMD, Mitchell EA. 2019. Nasal microbial composition and chronic otitis media with effusion: a case-control study. *PLoS One* 14:e0212473. <https://doi.org/10.1371/journal.pone.0212473>.
 81. De Boeck I, Wittouck S, Wuylts S, Oerlemans EFM, van den Broek MFL, Vandeneuvel D, Vanderveken O, Lebeer S. 2017. Comparing the healthy nose and nasopharynx microbiota reveals continuity as well as niche-specificity. *Front Microbiol* 8:2372. <https://doi.org/10.3389/fmicb.2017.02372>.
 82. de Steenhuijsen Pijters WA, Bogaert D. 2016. Unraveling the molecular mechanisms underlying the nasopharyngeal bacterial community structure. *mBio* 7:e00009-16. <https://doi.org/10.1128/mBio.00009-16>.
 83. Mandal S, Van Treuren W, White RA, Eggesbo M, Knight R, Peddada SD. 2015. Analysis of composition of microbiomes: a novel method for studying microbial composition. *Microb Ecol Health Dis* 26:27663. <https://www.tandfonline.com/doi/full/10.3402/mehd.v26.27663>.
 84. Krismer B, Liebeck M, Janek D, Nega M, Rautenberg M, Hornig G, Unger C, Weidenmaier C, Lalk M, Peschel A. 2014. Nutrient limitation governs *Staphylococcus aureus* metabolism and niche adaptation in the human nose. *PLoS Pathog* 10:e1003862. <https://doi.org/10.1371/journal.ppat.1003862>.
 85. Kandler O. 1983. Carbohydrate metabolism in lactic acid bacteria. *Antonie Van Leeuwenhoek* 49:209–224. <https://doi.org/10.1007/BF00399499>.
 86. Repka LM, Chekan JR, Nair SK, van der Donk WA. 2017. Mechanistic understanding of lanthipeptide biosynthetic enzymes. *Chem Rev* 117:5457–5520. <https://doi.org/10.1021/acs.chemrev.6b00591>.
 87. Dong SH, Tang W, Lukk T, Yu Y, Nair SK, van der Donk WA. 2015. The enterococcal cytolysin synthetase has an unanticipated lipid kinase fold. *Elife* 4:e07607. <https://doi.org/10.7554/eLife.07607>.
 88. Ramsey MM, Freire MO, Gabriliska RA, Rumbaugh KP, Lemon KP. 2016. *Staphylococcus aureus* shifts toward commensalism in response to *Corynebacterium* species. *Front Microbiol* 7:1230. <https://doi.org/10.3389/fmicb.2016.01230>.
 89. Hardy BL, Dickey SW, Plaut RD, Riggins DP, Stibitz S, Otto M, Merrell DS. 2019. *Corynebacterium pseudodiphtheriticum* exploits *Staphylococcus aureus* virulence components in a novel polymicrobial defense strategy. *mBio* 10:e02491-18. <https://doi.org/10.1128/mBio.02491-18>.
 90. Stubbendieck RM, May DS, Chevrette MG, Temkin MI, Wendt-Pienkowski E, Cagnazzo J, Carlson CM, Gern JE, Currie CR. 2018. Competition among nasal bacteria suggests a role for siderophore-mediated interactions in shaping the human nasal microbiota. *Appl Environ Microbiol* 85:e02406-18. <https://doi.org/10.1128/AEM.02406-18>.
 91. Claesen J, Spagnolo J, Flores Ramos S, Kurita K, Byrd A, Aksenov IA, Melnik A, Wong W, Wang S, Hernandez R, Donia M, Dorrestein P, Kong H, Segre J, Linington R, Fischbach M, Lemon K. 2019. *Cutibacterium acnes* antibiotic production shapes niche competition in the human skin microbiome. *bioRxiv* <https://doi.org/10.1101/594010>.
 92. Parlet CP, Brown MM, Horswill AR. 2019. Commensal staphylococci influence *Staphylococcus aureus* skin colonization and disease. *Trends Microbiol* 27:497–507. <https://doi.org/10.1016/j.tim.2019.01.008>.
 93. Otto M, Sussmuth R, Vuong C, Jung G, Gotz F. 1999. Inhibition of virulence factor expression in *Staphylococcus aureus* by the *Staphylococcus epidermidis* agr pheromone and derivatives. *FEBS Lett* 450:257–262. [https://doi.org/10.1016/s0014-5793\(99\)00514-1](https://doi.org/10.1016/s0014-5793(99)00514-1).
 94. Otto M, Echner H, Voelter W, Gotz F. 2001. Pheromone cross-inhibition between *Staphylococcus aureus* and *Staphylococcus epidermidis*. *Infect Immun* 69:1957–1960. <https://doi.org/10.1128/IAI.69.3.1957-1960.2001>.
 95. Iwase T, Uehara Y, Shinji H, Tajima A, Seo H, Takada K, Agata T, Mizunoe Y. 2010. *Staphylococcus epidermidis* Esp inhibits *Staphylococcus aureus* biofilm formation and nasal colonization. *Nature* 465:346–349. <https://doi.org/10.1038/nature09074>.
 96. Fritz SA, Hogan PG, Hayek G, Eisenstein KA, Rodriguez M, Epplin EK, Garbutt J, Fraser VJ. 2012. Household versus individual approaches to eradication of community-associated *Staphylococcus aureus* in children: a randomized trial. *Clin Infect Dis* 54:743–751. <https://doi.org/10.1093/cid/cir919>.
 97. Caporaso JG, Kuczynski J, Stombaugh J, Bittinger K, Bushman FD, Costello EK, Fierer N, Pena AG, Goodrich JK, Gordon JI, Huttley GA, Kelley ST, Knights D, Koenig JE, Ley RE, Lozupone CA, McDonald D, Muegge BD, Pirrung M, Reeder J, Sevinsky JR, Turnbaugh PJ, Walters WA, Widmann J, Yatsunenkov T, Zaneveld J, Knight R. 2010. QIIME allows analysis of high-throughput community sequencing data. *Nat Methods* 7:335–336. <https://doi.org/10.1038/nmeth.f.303>.
 98. Edgar RC, Haas BJ, Clemente JC, Quince C, Knight R. 2011. UCHIME improves sensitivity and speed of chimera detection. *Bioinformatics* 27:2194–2200. <https://doi.org/10.1093/bioinformatics/btr381>.
 99. Edgar RC. 2010. Search and clustering orders of magnitude faster than BLAST. *Bioinformatics* 26:2460–2461. <https://doi.org/10.1093/bioinformatics/btq461>.
 100. Caporaso JG, Bittinger K, Bushman FD, DeSantis TZ, Andersen GL, Knight R. 2010. PyNAST: a flexible tool for aligning sequences to a template alignment. *Bioinformatics* 26:266–267. <https://doi.org/10.1093/bioinformatics/btp636>.
 101. Eren AM, Morrison HG, Lescault PJ, Reveillaud J, Vineis JH, Sogin ML. 2015. Minimum entropy decomposition: unsupervised oligotyping for sensitive partitioning of high-throughput marker gene sequences. *ISME J* 9:968–979. <https://doi.org/10.1038/ismej.2014.195>.
 102. Callahan BJ, McMurdie PJ, Rosen MJ, Han AW, Johnson AJ, Holmes SP.

2016. DADA2: high-resolution sample inference from Illumina amplicon data. *Nat Methods* 13:581–583. <https://doi.org/10.1038/nmeth.3869>.
103. Wang Q, Garrity GM, Tiedje JM, Cole JR. 2007. Naive Bayesian classifier for rapid assignment of rRNA sequences into the new bacterial taxonomy. *Appl Environ Microbiol* 73:5261–5267. <https://doi.org/10.1128/AEM.00062-07>.
104. Malley R, Lipsitch M, Stack A, Saladino R, Fleisher G, Pelton S, Thompson C, Briles D, Anderson P. 2001. Intranasal immunization with killed unencapsulated whole cells prevents colonization and invasive disease by capsulated pneumococci. *Infect Immun* 69:4870–4873. <https://doi.org/10.1128/IAI.69.8.4870-4873.2001>.
105. Lemon KP, Klepac-Ceraj V, Schiffer HK, Brodie EL, Lynch SV, Kolter R. 2010. Comparative analyses of the bacterial microbiota of the human nostril and oropharynx. *mBio* 1:e00129-10. <https://doi.org/10.1128/mBio.00129-10>.